

This is an open access article distributed under the terms of the Creative Commons Attribution 4.0 International License (CC BY 4.0), which permits use, distribution, and reproduction in any medium, provided the original publication is properly cited. No use, distribution or reproduction is permitted which does not comply with these terms.

EXPERIMENTAL AND THEORETICAL PERFORMANCE EVALUATION OF BASIN SOLAR STILL WITH LID AFLOAT IN EGYPT CONDITIONS

Amr Mesalem , Ahmed Walaa , Ahmed Elweteedy , Salman Elshamarka

Military Technical College, Cairo, Egypt

*E-mail of corresponding author: amrmesalem@gmail.com

Resume

This paper presents experimental and theoretical work, analyzing the performance of single slope solar still with and without a floating lid, conducted in Cairo, Egypt. A Comparison of the experimental output yield with the theoretical one was carried out. The experimentations without the lid were conducted for 7 days and the daily output yield ranges from (2.8 l/day to 3.15 l/day) with an average output yield of 52.8 % when compared to the theoretical output yield. To improve the output yield of the still, a black fibrous lid was placed on the water surface and its effect on the output yield was studied. Because of its porosity the evaporation surface area of the still was improved, water depth is considered small above its surface. The experimentations with the lid were conducted for 6 days and the daily output yield ranges from (3.1 l/day to 3.3 l/day) with an average output yield of 57.95 % when compared to the theoretical yield.

Article info

Received 25 August 2021 Accepted 4 February 2022 Online 27 April 2022

Keywords:

single slope solar still passive type floating lid output yield heat transfer

Available online: https://doi.org/10.26552/com.C.2022.3.B199-B210

ISSN 1335-4205 (print version) ISSN 2585-7878 (online version)

1 Introduction

The Environment is composed of four main components Air, water, soil and energy. Without them there would be an environment, simply there would be life on earth. Water comes clearly in the second place after air for the existence of life. The water covers a huge area of the earth's surface, more than two-thirds of the earth's surface. About 97.5 % of water resources are found in seas and oceans which are not suitable for human consumption as they contain high salty water (3000 ppm to 35000 ppm) and the remaining 2.5 % are freshwater present in the lakes, rivers, polar ice and groundwater. So only a small portion of freshwater is being used in irrigation, industry and fulfilling the domestic demand.

The world is expected to face a problem of shortage of drinking water due to an increase in population and fast industrial development. Pollution of freshwater resources (rivers, lakes and underground water) by industrial wastes has enlarged the problem as well

One of the most sustainable solutions to provide fresh water for many communities is water desalination. Desalination is a process in which saline water is separated into two parts using various forms of energy, one that has a low concentration of dissolved salts (freshwater) and the other which has a much higher concentration of dissolved salts than the original feed water. Saline water is classified as either slightly salty water or brine water relying on the salinity and water source.

Most of the countries facing water shortage have large commercial desalination plants that use fossil fuel. Only some countries in the world can use fossil fuels to run these plants. But most of the countries have neither the financial nor oil resources to allow them to develop similarly. The production of 1000 m³ per day of freshwater requires 10,000 tonnes of oil per year [1], which can be considered a highly significant energy consumption, as it involves a recurrent energy expense. The cost of conventional desalination systems operating using fossil fuels keeps increasing due to the increase of world energy prices. Recently, the utilization of renewable energy sources to drive desalination plants appears to be very promising, as it is a sustainable, cheap and clean solution for freshwater supply in regions lacking energy resources. Recently, attention has been directed towards improving the coupling of solar energy systems and desalination technologies.

 ${
m B200}$ Mesalem et al.

Extensive research and activities have been conducted for the sake of reaching this goal.

There are two main types of solar still systems which are active solar still and passive solar still. In the active solar still, direct solar radiation and additional thermal energy are fed into the basin. Active distillation systems have been developed to increase the output of distilled water. Raju and Narayana [2] presented experimentally the effect of integrating of flat plate collector (FPC) with solar still. The result showed that connecting two FPCs in series with solar still, provides 41 % more distilled water when compared to a single FPC. Singh et al. [3] discussed the improvement in the performance of a solar still integrated with an evacuated tube collector and showed that the best combination has been attained by integrating 10 evacuated tubes with a water depth of 3 cm with a maximum daily output yield

of 3.8 kg/m². Sampathkumar et al. [4] discussed the performance of various active solar distillation systems.

In the passive solar still, the water in the basin is heated by solar radiation directly so that the productivity is very low compared to the active solar still. The daily output yield of passive solar still can be increased by changing the design of the conventional still (single slope) or by making modifications in the conventional design. et al. [5] made a comparison between the output yield of triangular basin solar still (TBSS) and conventional basin solar still (CBSS), the experiment revealed that the daily output yield obtained from CBSS and TBSS was found to be 2.7 and 3.2 kg/m², respectively. In addition, the daily efficiency of the TBSS was improved by 11.36 % than the CBSS.

et al. [6] designed and fabricated concave type solar still with four glass cover surface (Pyramid shape)

Table 1 Modifications on conventional solar still

Reference	Modification	Results
Matrawy et al. [12]	Formed the evaporative surface as a corrugated shape.	Improvement of about 34 % in the productivity.
	Decreased the heat capacity by using porous material.	
Abdallah et al. [13]	Discussed the effect of various absorbing materials on the thermal performance of solar stills.	Distilled water collections were 28 %, 43 % and 60 % for coated and uncoated metallic wiry sponges and black rocks respectively.
	Materials: black coated and uncoated metallic wiry sponges and black rocks.	
Srivastava and	Modification is made by incorporating	Increase in the evaporation surface area.
Agrawal [14]	multiple low thermal inertia porous absorbers, floated adjacent to each other.	On clear days 68 $\%$ more distillate output was obtained.
		35 % more on cloudy days
Agrawal and Rana [15]	Multiple V-shaped floating wicks are used to enhance the heat absorption and thereby increase productivity.	The evaporative surface area of modified solar still is 26 % larger than that of the conventional one.
		The maximum daily productivity in one of the clear days is found to be approximately 6.20 kg/m2 in summer and 3.23 kg/m2 in winter with daily efficiencies of 56.62 % and 47.75 %, respectively.
Gawande and Bhuyar [16]	Discussed the Effect of Shape of the Absorber Surface on the Performance of Stepped Type Solar Still.	When the convex and concave type, the average daily water production is 56.60 % and 29.24 % higher than that of flat type.
	The shape of the absorber surface provided in the basins of solar stills was flat, convex and concave.	
Johnson et al. [17]	Performed a theoretical and experimental study on a single-basin solar still when an external solar enhancement is used (Fresnel	A parametric study by varying the water depth showed the Fresnel lens was more effective for larger water depths.
	lens).	The Fresnel lens can aid in improving the overall efficiency of the solar still.
Gupta et al. [18]	Studied the performance of modified solar still using the water sprinkler. Attachment of water sprinkler with constant water flow rate of 0.0001 kg/s on the glass cover.	The distilled water output was recorded 2940 ml and 3541 ml from conventional and modified solar stills, respectively.
		Water productivity (output yield) of single slope solar still is increased by 20 %.
		The overall efficiency is increased by 21 $\%$ over the conventional solar still.

and studied it experimentally. The results show that the average productivity during the daytime is 4 l/m² with a system efficiency of 0.38, higher than the conventional type solar still. Arunkumar et al. [7] made an experimental study on hemispherical solar still which has a higher efficiency than the conventional solar still and compared the daily distillate output with and without flowing water over the cover The efficiency was 34 % and increased to 42 % with the top cover cooling effect (flowing water). Jathar et al. [8] investigated experimentally a concave-type solar still with different temperature and solar intensity and it was noted that The highest daily productivity (3.7 l/m²/ day) was achieved during march 2020. This may be attributable to the highest average intensity of the radiation (1005 W/m²) and the most top average temperature difference of 10.5 °C. Gad et al. [9] manufactured and compared the experimental results of conical solar still to the conventional type with the same area. The results showed that the daily productivity for conical and conventional solar stills were 3.38 and 1.93 L/m²/day, respectively. Many researchers made modifications to the conventional solar still, to increase the output yield even more. Table 1 shows the recent modifications in conventional solar still.

In addition, many researches modifications in conventional solar still concerning different parameters and their effects on the yield. Many parameters affect the evaporation rate. Studying the effect of these parameters helped in increasing the evaporation rate. Hence, better yield. One of these parameters is the water depth; it was found out that the evaporation rate is inversely proportional to water depth. grawal et al. [10] made an experimental and theoretical comparison of the daily output yield for different water depths from 200 mm and 10 mm. the experimental value for daily efficiency was around 41.49 % and 32.42 % respectively. It is obvious that to achieve a higher efficiency of a solar still, the heat loss should be minimized by adequate insulation. Khalifa and Hamood [11] studied experimentally the effect of insulation thickness on the productivity of solar still and developed a performance correlation for the effect of insulation on the productivity. Their study showed that the insulation thickness could influence the productivity of the still by over 80 %.

In this paper, a detailed theoretical and experimental work is done on a solar still to get the hourly and daily yield. The work is conducted in the Military Technical College (MTC), Cairo, Egypt. The paper is organized as follows: first, a detailed thermal analysis for a solar still was performed to get the productivity. Then, a physical model for the solar still with net dimensions 1 m * 1 m is constructed. The experimental work was conducted for several days for the solar still with and without a floating lid on the water surface to compare both theoretical and experimental evaluation. Finally, results, discussion and conclusion are introduced.

2 Solar still thermal analysis

A thermal energy balance has been made for the solar still. The following assumptions are considered to simplify the analysis:

- The physical properties of water remain constant with temperature changes.
- Water vapor and dry air are assumed to be ideal gases.
- The outer temperature of the glass equals the inner temperature of the glass.
- The still is assumed to be completely vapor leakage proof.

2.1 Energy balance equations glass cover, water mass and basin linear [10]

The glass receives heat from internal and external sources by different methods, externally from the incident solar radiation and internally from basin water surface through three methods (convection, evaporation and radiation) and reject the received heat to the atmosphere through two methods (convection and radiation).

$$\alpha_g' I(t) + q_{twg} = g_{tga}, \qquad (1)$$

where.

$$q_{twg} = q_{cwg} + q_{ewg} + q_{rwg}, (2)$$

$$q_{tga} = q_{cga} + q_{rga}, (3)$$

$$\alpha'_{g} I(t) + h_{twg}(T_{w} - T_{g}) = h_{tga}(T_{g} - T_{a}).$$
 (4)

The basin water absorbs energy released from the basin liner and consumes it in two ways, some energy is stored in the water due to its specific heat and the rest is transferred to the glass cover through three methods (convection, evaporation and radiation).

$$\alpha'_{w} I(t) + q_{cbw} = q_{twg} + m_{w} c_{w} \left(\frac{dT_{W}}{dt}\right), \tag{5}$$

$$\alpha'_{w} I(t) + h_{cbw}(T_{b} - T_{w}) = h_{twg}(T_{w} - T_{g}) + m_{w}c_{w}\left(\frac{dT_{w}}{dt}\right).$$
(6)

The basin linear absorbs heat energy from the solar radiation transmitted from the glass and releases this energy to the basin water and the rest to the atmosphere by conduction and convection through walls of the still.

$$\alpha_b' I(t) = q_{chw} + q_{tha}, \tag{7}$$

$$\alpha'_{b} I(t) = h_{cbw}(T_{b} - T_{w}) + h_{tba}(T_{b} - T_{a}).$$
 (8)

m B202

By solving Equations (4), (6), (8) one gets,

$$\left(\frac{dT_w}{dt}\right) + aT_w = f(t), \tag{9}$$

where:

$$a = U_L/(m_w c_w), \ f(t) = M I(t) + a T_a, \ M = (\alpha'_{eff} h_{cbw})/m_w c_w (h_{cbw} + h_{tba}).$$

The solution of Equation (9) is

$$T_w = \left(\frac{f(t)}{a}\right)(1 - e^{at}) + Tw_0 e^{-at}.$$
 (10)

The hourly yield equals,

$$M_w = \left(\frac{h_{ewg} (T_w - T_g) * 3600}{L_{ev}}\right) * A_b.$$
 (11)

To solve the above equations heat transfer analysis for all solar still should be calculated. Equations from (12) to (42) will introduce the heat transfer analysis. Section three introduces the calculation methodology.

The latent heat of evaporation is calculated by [19],

$$L_{ev} = (2501.67 - 2.389 * T_w) * 10^3.$$
 (12)

2.2 Solar still heat transfer analysis

There are mainly two types of heat transfers taking place in the process of solar still (Internal and external)

Internal heat transfer

It occurs between the basin water surface and inner glass cover through three methods (convection, evaporation and radiation).

The convection heat transfer between the water and the inner glass cover is calculated from,

$$q_{cwg} = h_{cwg}(T_w - T_g). \tag{13}$$

Empirical relation for the convection heat transfer coefficient is given by Dunkle [20].

$$h_{cwg} = 0.884 \left[(T_w - T_g) + \frac{(P_w - P_g)(T_w + 273)}{(268.9 * 10^3 - P_w)} \right]^{1/3}$$
. (14)

The evaporation heat transfer between water and inner glass cover is calculated from,

$$q_{ewg} = h_{ewg}(T_w - T_g), (15)$$

$$h_{ewg} = \frac{16.28 * 10^{-3} * h_{cwg} (P_w - P_g)}{(T_w - T_g)}.$$
 (16)

The radiation heat transfer between water and inner glass cover is calculated from,

$$q_{rwg} = h_{rwg}(T_w - T_g). (17)$$

In addition, given by Stefan Boltzmann's equation:

$$q_{rwg} = \varepsilon_{eff} \sigma [(T_w + 273)^4 - (T_g + 273)^4].$$
 (18)

From Equations (17) and (18):

$$h_{rwg} = \frac{\varepsilon_{eff} \sigma [(T_w + 273)^4 - (T_g + 273)^4]}{(T_w - T_g)}.$$
 (19)

Finally, the total internal heat transfer coefficients are:

$$h_{twa} = h_{cwa} + h_{ewa} + h_{rwa}$$
 (20)

External heat transfer

External heat transfer is contributed by the top, bottom and sides losses of the solar still.

Top heat losses occur between the outer glass cover and the atmosphere through two methods (convection and radiation).

The radiation heat transfer is

$$q_{rga} = h_{rga} (T_g - T_{sky}), (21)$$

$$q_{rga} = \varepsilon_g \sigma [(T_g + 273)^4 - (T_{sky} + 273)^4].$$
 (22)

From Equations (21) and (22)

$$h_{rga} = \frac{\varepsilon_g \sigma [(T_g + 273)^4 - (T_{sky} + 273)^4]}{(T_g - T_{sky})}.$$
 (23)

The sky temperature is estimated from [21]:

$$T_{sky} = 0.0552 * T_a^{1.5}. (24)$$

The convective heat transfer is

$$q_{cga} = h_{cga} (T_g - T_a). (25)$$

where from [22]

$$h_{cga} = 2.8 + 3.0 V_w, (26)$$

if
$$V_w \le 5 \, m/s \& 6.15 * (V_w)^{0.8}$$
 if $V_w > 5 \, m/s$.

Finally, the total top heat transfer coefficients are

$$h_{tga} = h_{cga} + h_{rga}. (27)$$

The bottom and side heat losses occur between the water in the basin and the outer atmosphere through the insulation on the sides and base through three methods (conduction, evaporation and radiation).

$$q_{tba} = h_{tba}(T_b - T_a). (28)$$

Table 2 Attenuation (Att) factors for varying water depth

d _w (m)	Attenuation factor	
0.02	0.6756	
0.03	0.6441	
0.04	0.6185	
0.05	0.6124	
0.06	0.5858	
0.08	0.5648	
0.10	0.5492	

Table 3 Design parameters

Parameters	Numerical values
Basin area, A _b	1 m ²
Glass absorptivity, α_g	0.04
Glass reflectivity, R_g	0.06
Glass emissivity, $\varepsilon_{_{\mathrm{g}}}$	0.9
Water reflectivity, $R_{\rm w}$	0.05
Water emissivity, $ \varepsilon_{_{ m w}} $	0.95
Water heat capacity, $c_{_{\rm w}}$	4180 J/kg K
Time, t	3600 s
The thickness of glass cover, $L_{_{\rm g}}$	0.008 m
Glass thermal conductivity, $K_{_{\rm g}}$	1.03 W/m K
The thickness of insulation, $L_{_{\rm i}}$	0.02 m
Insulation thermal conductivity, K_{i}	0.035 w/m K
Stefan Boltzmann's constant, σ	$5.6697*10^{-8} \text{ w/m}^2.\text{K}^4$
${ m h_w}$	$250~\mathrm{W/m^2~K}$
Water depth, d	0.03 m
$ m h_{_{ba}}$	2.8 W/m ² °C
h	250 W/m ² °C (summer)
$h_{ m cbw}$	200 W/m ² °C (winter)

The heat loss coefficient from basin liner to the atmosphere

$$h_{tba} = \left[\left(\frac{L_i}{K_i} \right) + \left(\frac{1}{h_{ba}} \right) \right]^{-1}, \tag{29}$$

where:

$$h_{ba} = h_{rba} + h_{cba}. ag{30}$$

Side heat loss is,

$$h_{sa} = h_{tba} * \left(\frac{A_s}{A_b}\right). \tag{31}$$

Solar radiation fractions [23]

The water temperature $T_{_{\rm w}}$ and the glass temperature $T_{_{\rm g}}$ depend on the solar radiation fractions, which are defined as the fraction of solar energy absorbed for both water and glass.

The fraction absorbed by glass cover is

$$\alpha_g' = (1 - R_g)\alpha_g. (32)$$

The fraction absorbed by water without attenuation factor is,

$$\alpha'_w = (1 - \alpha g)(1 - R_g)(1 - R_w)\alpha_w.$$
 (33)

The fraction absorbed by water with attenuation factor is,

$$\alpha'_{w} = (1 - \alpha g)(1 - R_{g})(1 - R_{w})\alpha_{w} *[1 - \sum \mu_{j} EXP(-n_{j}d_{w})],$$
(34)

where, $\left[1-\sum \mu_j EXP(-n_j d_w)\right]$ is the attenuation factor that depends on water depth [20]. Table 2 represents the attenuation factor variation.

Then, the glass temperature is

$$T_{gi} = \frac{\alpha'_g \ I(t) + h_{twg} * T_w + U_{tga} * T_a}{h_{twg} + U_{Tga}},$$
 (35)

where, $U_{\mbox{\tiny Tra}a}$ is calculated from:

$$U_{Tga} = \frac{\frac{K_g}{L_g} * h_{tga}}{\frac{K_g}{L_g} + h_{tga}}.$$
 (36)

and the partial vapor pressures from:

$$P_w = EXP \left\{ 25.317 - \frac{5144}{(T_w + 273)} \right\},\tag{37}$$

$$P_g = EXP \left\{ 25.317 - \frac{5144}{(T_g + 273)} \right\}. \tag{38}$$

Finally, the overall heat transfer coefficients can be calculated from

calculated from
$$U_T = \frac{h_{twg} * U_{Tga}}{h_{twg} + U_{Tga}},$$
 (39)

$$U_b = \frac{h_w * h_{ba}}{h_w + h_{ba}},\tag{40}$$

$$U_{ss} = \left(\frac{A_{ss}}{A_b}\right) U_b \,, \tag{41}$$

$$U_L = U_b + U_t + U_{ss}. (42)$$

The above equations were set and solved by computer using the excel software to get the yield. The design parameters used are given in Table 3.

3 Calculation methodology

A certain procedure must be followed to compute the hourly heat transfer coefficients, water temperature, glass temperature and productivity.

1. First of all, water temperature, glass temperature, ambient temperature, solar radiation intensity and wind velocity must be measured and use these values to evaluate the partial vapor pressures $P_{\rm w}$ & $P_{\rm g}$ Equations (36) and (37), convection heat transfer coefficient between water and glass $h_{\rm rwg}$ Equation (14), evaporation heat transfer coefficient between water and glass $h_{\rm two}$ Equation (16), radiation

heat transfer coefficient between water and glass h_{rwg} Equation (19) and then deduce the total heat transfer coefficient between water and glass h_{ewg} Equation (20).

- 2. Use the value of h_{twg} to get the value of overall heat transfer coefficients Equations (38) to (41) from these values calculate the new value of T_w .
- 3. From evaporation heat transfer coefficient $h_{_{\rm ewg}}$ calculate the hourly yield $M_{_{\rm w}}$ from Equation (11).
- 4. From the value of $T_{\rm w}$ get a new value of $T_{\rm g}$ Equation (34) and repeat the previous steps.

Experimental work

The solar still is designed and constructed to compare the productivity with and without the floating lid. The work is conducted in Military Technical College (MTC), Cairo, Egypt (Latitude: 30, Longitude: 31). The solar still takes the design of a box with dimensions of 1.3 m length, 1.1 m breadth and 0.9 m height. The box is made of plywood with 0.05 m thickness. It has four sides, two of these sides are rectangular and the other two are trapezoidal. The area available for water is 1 m * 1 m. The basin has three holes one for feeding water, one for impure water outlet and the third for distilled water output. The outside walls are insulated with glass wool with thermal conductivity K = 0.035 w/mK. The distillate channel is covered with polyester fabric with a slope of 1/10 to ease the flow of distilled water through the hole to reach the graduated flask insulated with the same material as still. The distilled water passes from the PVC pipe to the flask through a U-tube which acts as a manometer to prevent any air from entering the still. The condensing surface is a normal glass with a thickness of 8 mm, emissivity = 90 %, reflectivity = 6 % and absorptivity = 4 \%. The glass is inclined at an angle of 30°, which is equal to the latitude of Cairo. Silicon rubber was used to fill the gaps between plywood edges. The basin was coated with black painted polyester fabric to enhance the absorptivity of solar radiation. Figure 1 shows the constructed physical model. Figure 2 shows the instruments used in the experiment. Figure 3



Figure 1 Photograph of the constructed solar still

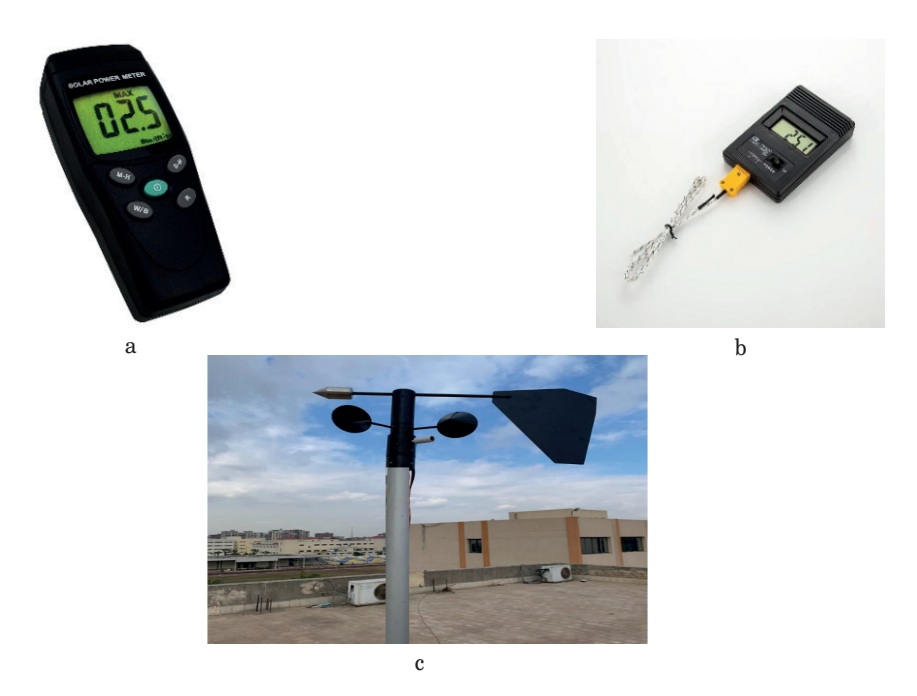


Figure 2 Instruments for experimentation: a-solar power meter, b- digital thermometer, c- wind speed meter

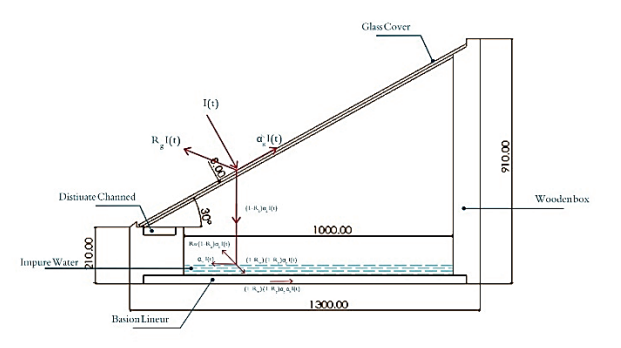


Figure 3 Schematic diagram of the solar radiation

shows the schematic diagram of solar radiation in the experiment and the main parts of the solar still.

The experimental work was conducted for two cases; solar still without the lid and solar still with the lid afloat.

For the solar still without lid afloat, the experiments were conducted for seven days of the summer season, 2021 from July 1st to July 7th. The still was placed in the south direction. Solar radiation intensity was measured by using a pyrometer. Wind velocity was taken from the website: timeanddate.com and compared to the measured velocity in MTC and the two readings are the same. These data were used in the theoretical calculation. Both water temperature and glass cover temperature were measured with Ni/Cr electric thermometer and were compared to the theoretical values. The water depth was set to be 30 mm at the beginning of each experimental day. The condensed water was collected in a graduated flask. The yield was considered every 24 hours starting at 7:00 am. The measured solar radiation intensity

range was (0 to 990.8 w/m^2) and wind velocity was (0 to 7.78 m/s).

For the solar still with the lid afloat, the experiments were conducted for six days starting from July $8^{\rm th}$ to July $13^{\rm th}$. A black fibrous lid was placed on the surface of the water. The distilled water was measured every 24 hours starting from 7:00 am. Solar radiation intensity range was taken as (0 to $989.7~{\rm w/m^2}$) and wind velocity was taken as (1.11 to $7.78~{\rm m/s}$).

5 Results and discussion

The outputs of the experiment were recorded and compared to the theoretical values, by following the methodology of calculations in section 3.

Figure 4 shows the ambient and sky temperature along the first day of experimentation, which is used in calculations to get the output yield. The ambient temperature was in the range from $26~^{\circ}\mathrm{C}$ to $38~^{\circ}\mathrm{C}$.

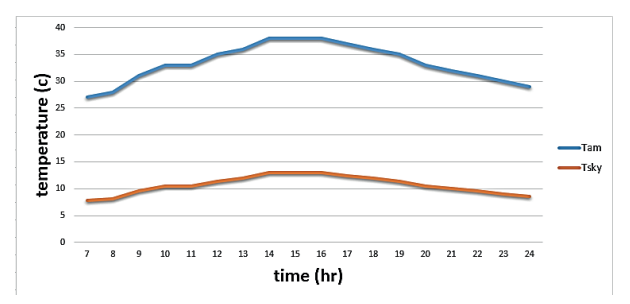


Figure 4 Ambient and sky temperature from for the first day of calculations (1-7-2021)

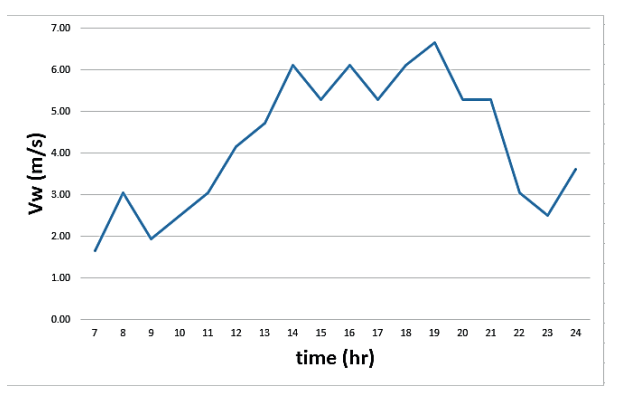


Figure 5 Wind velocity from the website for the first day of calculations (1-7-2021)

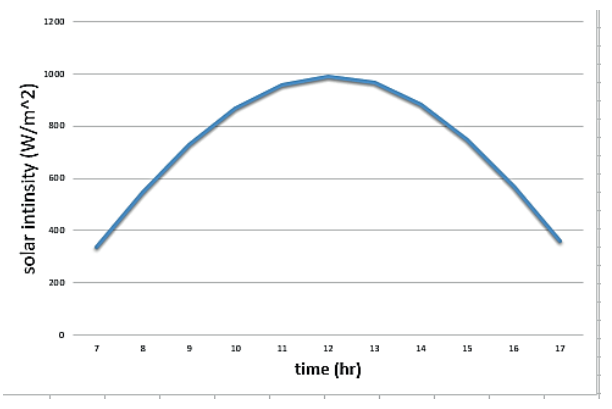


Figure 6 The solar intensity measured by pyrometer on the first day of calculations (1-7-2021)

Figure 5 shows the wind velocity variation along the day. For the first experimental day, it varies from 4.2 to 6.8 m/s.

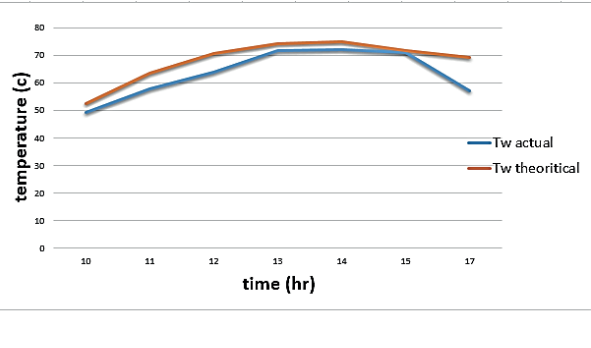
Figure 6 shows the solar radiation intensity measured along the day. It varies from 390 to 999 $\mbox{W/m}^2.$

Figure 7 shows the difference between the measured and theoretical temperatures of both water and glass. The difference between both ranged from 3 to 5 $^{\circ}$ C.

Figure 8 shows the variation of latent heat of vaporization along the day.

Figure 9 shows the variation of different heat transfer coefficients. It gives a relation between the heat transfer coefficient between the water and glass and the time along the day.

Figure 10 shows the hourly yield output throughout the day. It gives the relation between the hourly yield



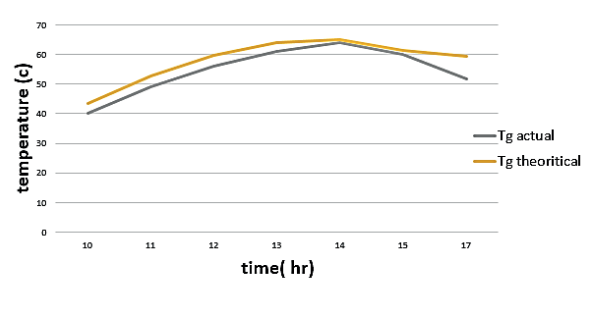


Figure 7 The temperature comparison between the actual and theoretical water and glass temperatures on the first day of calculations (1-7-2021)

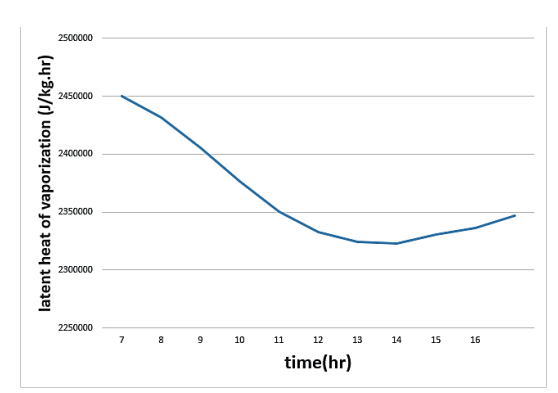


Figure 8 The variation of latent heat of vaporization with the hours of the day

and the time of the day. Its value 0.012 l/m^2hr at 7:00 am and reaches a peak of 0.92 L/m^2hr at 1:00 pm with an accumulated value of 5.6 l/m^2 .day.

Figure 11 shows the difference between the actual and the theoretical yield of the solar still. It shows that the average actual yield is about 52 % of the theoretical yield. Theoretical daily output is higher than the experimental values due to different heat losses from the still.

For the solar still with a floating lid, the experimental output yield values were compared to the results obtained without the floating lid to indicate the effect of the floating lid on the productivity of the solar still. Figure 12 shows the comparison. It was found that the ratio increased to 58 % with about 6 % of the first condition. This is due to the porosity of the lid; the evaporative surface area of the still was increased.

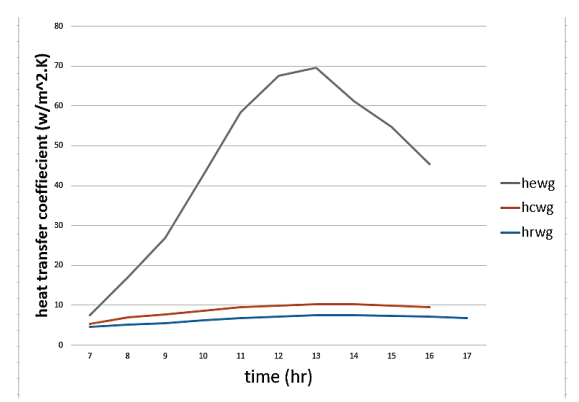


Figure 9 The variation of heat transfer coefficients between water and glass along the time of the day

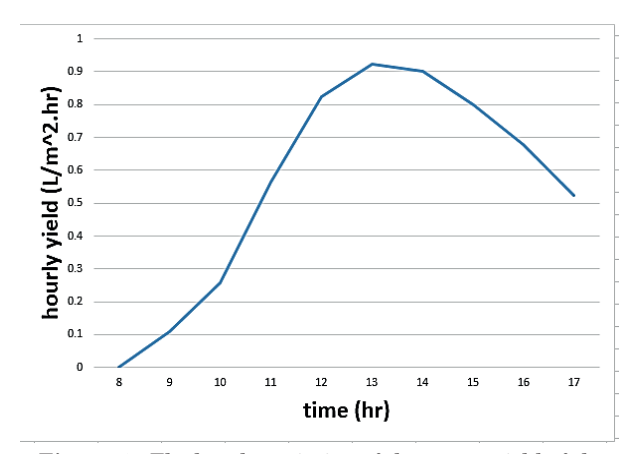


Figure 10 The hourly variation of the output yield of the solar still along this day

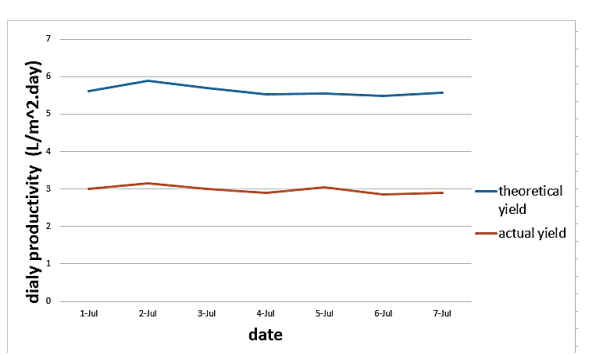


Figure 11 Yield comparison without a lid on seven days from (July 1st to July 7th) shows that the actual yield is about 52 % of the theoretical yield

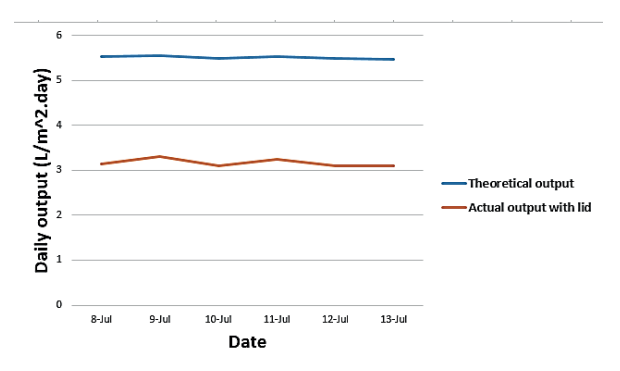


Figure 12 Yield comparison with a lid on six days from (July 8th to July 13th) shows that the actual yield is about 58 % of the theoretical yield

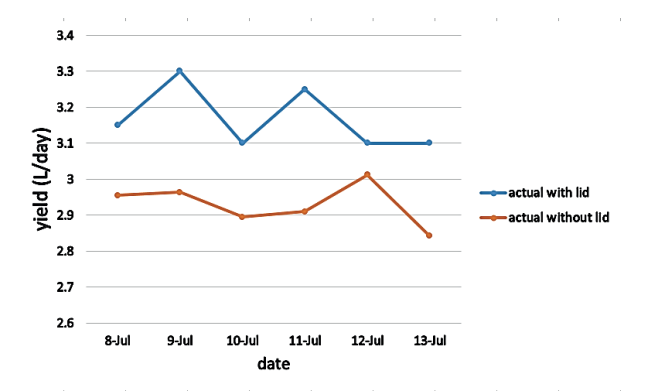


Figure 13 Comparison between the actual yield with lid and the actual yield without lid

Figure 13 shows the effect of using a lid afloat and the comparison between the actual yield with and without the lid.

6 Conclusions

The single slope solar still was fabricated and investigated. Different parameters as glass temperature, water temperature and output yield were measured and compared to the theoretically calculated values. In addition, this work shows the effect of placing a floating

lid (black fibrous lid) which is porous material on the output yield of the solar still. The output yield of the still with a floating lid was compared to the ratio of the experimental and theoretical output yield. It was found that:

- 1. The output without a lid was 52 % of the theoretical output.
- 2. The output with lid was 58 % from the theoretical output.
- 3. Placing a porous material on the surface of the water increased the productivity by 6 % of the regular output.

4. The porous material works as a heat absorber and increases the evaporative area of water because of

the surface area of water balls that pass throw the holes of the material by capillary effect.

References

- [1] KALOGIROU, S. A. Seawater desalination using renewable energy sources. *Progress in Energy and Combustion Science* [online]. 2005, **31**(3), p. 242-281. ISSN 0360-1285. Available from: https://doi.org/10.1016/j.pecs.2005.03.001
- [2] RAJU, V. R., NARAYANA, R. L. Effect of flat plate collectors in series on performance of active solar still for Indian coastal climatic condition. *Journal of King Saud University - Engineering Sciences* [online]. 2015, 30(1), p. 78-85. ISSN 1018-3639. Available from: https://dx.doi.org/10.1016/j.jksues.2015.12.008
- [3] SINGH, R. V., KUMAR, S., HASAN, M. M., KHAN, M. E., TIWARI, G. N. Performance of a solar still integrated with evacuated tube collector in natural mode. *Desalination* [online]. 2013, **318**, p. 25-33. ISSN 0011-9164. Available from: https://doi.org/10.1016/j.desal.2013.03.012
- [4] SAMPATHKUMAR, K., ARJUNAN, T. V., PITCHANDI, P., SENTHILKUMAR, P. Active solar distillation a detailed review. Renewable and Sustainable Energy Reviews [online]. 2010, 14(6), p. 1503-1526. ISSN 1364-0321. Available from: https://doi.org/10.1016/j.rser.2010.01.023
- [5] PRASAD, A. R., SATHYAMURTHY, R., SUDHAKAR, M., MADHU, B., MAGESHBABU, D., MANOKAR, A. M., CHAMKHA, A. J. Effect of design parameters on fresh water produced from triangular basin and conventional basin solar still. *International Journal of Photoenergy* [online]. 2021, 2021, 6619138. ISSN 1110-662X, eISSN 1687-529X. Available from: https://doi.org/10.1155/2021/6619138
- [6] PRADEE, M., VEMBATHURAJESH, A., SUNDARAM, C. M., SIVAGANESAN, V., NAGARAJAN, B. Design, fabrication and performance analysis of concave solar still. In: 2013 IEEE Energytech: proceedings [online]. IEEE. 2013. eISBN 978-1-4673-4444-9. Available from: https://doi.org/10.1109/EnergyTech.2013.6645306
- [7] ARUNKUMAR, T., JAYAPRAKASHA, R., DENKENBERGER, D., AHSAN, A., OKUNDAMIYA, M. S., KUMAR, S., TANAKA, H., AYBARG, H. S. An experimental study on a hemispherical solar still. *Desalination* [online]. 2012, **286**, p. 342-348. ISSN 0011-9164. Available from: https://doi.org/10.1016/j.desal.2011.11.047
- [8] JATHAR, L. D., GANESAN, S., GORJIAN, S. An experimental and statistical investigation of concave-type stepped solar still with diverse climatic parameters. *Cleaner Engineering and Technology* [online]. 2021, 4, 100137. ISSN 2666-7908. Available from: https://doi.org/10.1016/j.clet.2021.100137
- [9] GAD, H. E., EL-DIN, S. S., HUSSIEN, A. A., RAMZY, K. Thermal analysis of a conical solar still performance: an experimental study. *Solar Energy* [online]. 2015, **122**, p. 900-909. ISSN 0038-092X. Available from: https://doi.org/10.1016/j.solener.2015.10.016
- [10] AGRAWAL, A., RANA, R. S., SRIVASTAVA, P. K. Heat transfer coefficients and productivity of a single slope single basin solar still in Indian climatic condition: experimental and theoretical comparison. *Resource - Efficient Technologies* [online]. 2017, 3(4), p. 466-482. ISSN 2405-6537. Available from: https://doi.org/10.1016/j. reffit.2017.05.003
- [11] KHALIFA, A. J. N., HAMOOD, A. M. Effect of insulation thickness on the productivity of basin type solar stills: an experimental verification under local climate. *Energy Conversion and Management* [online]. 2009, **50**(9), p. 2457-2461. ISSN 0196-8904. Available from: https://doi.org/10.1016/j.enconman.2009.06.007
- [12] MATRAWY, K. K., ALOSAIMY, A. S., MAHROUS, A. F. Modeling and experimental study of a corrugated wick type solar still: comparative study with a simple basin type. *Energy Conversion and Management* [online]. 2015, **105**, p. 1261-1268. ISSN 0196-8904. Available from: https://doi.org/10.1016/j.enconman.2015.09.006
- [13] ABDALLAH, S., ABU-KHADER, M. M., BADRAN, O. Effect of various absorbing materials on the thermal performance of solar stills. *Desalination* [online]. 2009, **242**(1-3), p. 128-137. ISSN 0011-9164. Available from: https://doi.org/10.1016/j.desal.2008.03.036
- [14] SRIVASTAVA, P. K., AGRAWAL, S. K. Experimental and theoretical analysis of single sloped basin type solar still consisting of multiple low thermal inertia floating porous absorbers. *Desalination* [online]. 2013, 311, p. 198-205. ISSN 0011-9164. Available from: https://doi.org/10.1016/j.desal.2012.11.035
- [15] AGRAWAL, A., RANA, R. S. Theoretical and experimental performance evaluation of single-slope single-basin solar still with multiple V-shaped floating wicks. *Heliyon* [online]. 2019, 5(4), e01525. eISSN 2405-8440. Available from: https://doi.org/10.1016/j.heliyon.2019.e01525
- [16] GAWANDE, J. S., BHUYAR, L. B. Effect of shape of the absorber surface on the performance of stepped type solar still. *Energy and Power Engineering* [online]. 2013, **5**(8), p. 489-497. ISSN 1949-243X, eISSN 1947-3818. Available from: https://doi.org/10.4236/epe.2013.58053

- [17] JOHNSON, A., MU, L., PARK, Y. H., VALLES, D. J., WANG, H., XU, P., KOTA, K., KURAVI, S. A thermal model for predicting the performance of a solar still with fresnel lens. Water [online]. 2019, 11(9), 1860. eISSN 2073-4441. Available from: https://doi.org/10.3390/w11091860
- [18] GUPTA, B., SHARMA, R., SHANKAR, P., BAREDAR, P. Performance enhancement of modified solar still using water sprinkler: an experimental approach. *Perspectives in Science* [online]. 2016, **8**, p. 191-194. ISSN 2213-0209. Available from: https://doi.org/10.1016/j.pisc.2016.04.029
- [19] FATH, H. E. S., HOSNY, H. M. Thermal performance of a single-sloped basin still with an inherent built-in additional condenser. *Desalination* [online]. 2002, 142(1), p. 19-27. ISSN 0011-9164. Available from: https://doi.org/10.1016/S0011-9164(01)00422-2
- [20] DUNKLE, R. Solar water distillation: the roof type still and the multiple effect diffusor still. In: International Developments in Heat Transfer ASME: proceeding. Part V. 1961. p. 895.
- [21] PEARCE, J. M., Denkenberger, D. Numerical simulation of the direct application of compound parabolic concentrators to a single effect basin solar still. In: 2006 International Conference of Solar Cooking and Food: proceedings. 2006.
- [22] WATMUFF, J. H., CHARTERS, W. W. S., PROCTOR, D. Solar and wind induced external coefficients solar collectors. 1977.
- [23] TIWARI, A. K., TIWARI, G. N. Thermal modeling based on solar fraction and experimental study of the annual and seasonal performance of a single slope passive solar still: the effect of water depths. *Desalination* [online]. 2007, **207**, p. 184-204. ISSN 0011-9164. Available from: https://doi.org/10.1016/j.desal.2006.07.011

Annex - Nomenclatures

- $A_{\scriptscriptstyle L}$ Basin liner surface area of the still (m²)
- A. Basin sidewall area of the still (m²)
- A_{a} Area of the solar still (m²)
- $q_{\mbox{\tiny cba}}$. Convective heat transfer from the bottom of the basin to ambient (W/ m²)
- $q_{\mbox{\scriptsize rba}}$ Radiative heat transfer from the bottom of the basin to ambient (W/ m²)
- $q_{\scriptscriptstyle cuss}$ Convective heat transfer from the basin water to glass cover (W/ m^2)
- $q_{\mbox{\tiny ewg}}$ Evaporative heat transfer from the basin water to glass cover (W/ m²)
- $q_{\mbox{\tiny rwg}}$ Radiative heat transfer from the basin water to glass cover (W/ m²)
- $q_{_{\mathit{hno}}}$ Total heat transfer from the basin water to glass cover (W/ $\mathrm{m}^2)$
- $q_{{\scriptscriptstyle cga}}$. Convective heat transfer from the glass cover to ambient (W/ m²)
- q_{rga}^{-} Radiative heat transfer from the glass cover to ambient (W/ m²)
- $q_{{\it tga}}^{-}$ Total heat transfer from the glass cover to ambient (W/ m²)
- $q_{\it cbw}^{\it o}$. Convective heat transfer from the basin liner to water (W/ m²)
- $q_{\it tba}$ $\,$ Total heat transfer from the basin liner to ambient (W/ $\rm m^2)$
- $q_{\it ba}$ $\,$ Total heat transfer from the bottom of the basin to ambient (W/ m²)
- R_a Reflectivity of the glass cover
- $\vec{R}_{...}$ Reflectivity of the basin water
- R_b Reflectivity of the basin liner
- h_{max}^{o} Convective heat transfer coeffcient from the basin water to glass cover (W/m² °C)
- $h_{_{one}}$ Evaporative heat transfer coeffcient from the basin water to glass cover (W/m 2 °C)
- h_{rwg} Radiative heat transfer coeffcient from the basin water to glass cover (W/m²°C)
- Radiative heat transfer coeffcient from the basin water to glass cover (W/m 2 °C)
- h_{coa} Convective heat transfer coeffcient from the glass cover to ambient (W/m² °C)
- h_{rga} Convective heat transfer coeffcient from the glass cover to ambient (W/m²°C)
- h_{*aa} Total heat transfer coeffcient from the glass cover to ambient (W/m² °C)
- h_{chw} Convective heat transfer coeffcient from the basin liner to water (W/m² °C)
- Total heat transfer coeffcient from the basin liner to ambient (W/m 2 °C)
- $h_{\rm la}$ Total heat transfer coeffcient from the bottom of the basin to ambient (W/m²°C)
- $h_{\rm star}$ Convective heat transfer coeffcient from the bottom of the basin to ambient (W/m²°C)
- $h_{\rm de}$ Radiative heat transfer coeffcient from the bottom of the basin to ambient (W/m²°C)
- h_{∞} side heat transfer coefficient (W/m2°C)
- U_b Overall bottom heat transfer coeffcient from bottom to ambient (W m 2 °C)
- $U_{\tau_{m}}^{\circ}$ Overall heat transfer coefficient from glass to ambient (W/m² °C)
- U, Overall top heat transfer coeffcient from basin water to ambient (W/m² °C)
- U_{L} Overall heat transfer coeffcient for still (W m² °C)

- $U_{\rm \scriptscriptstyle SS}$ –Overall side heat transfer coefficient between water and surrounding (W/m² °C)
- T Glass cover temperature (°C)
- T_{b}^{g} Basin water temperature (°C)
- T_a Ambient temperature (°C)
- T_b^a Basin liner temperature (°C)
- T_{obs} Sky temperature (°C)
- V_{m} Velocity of Wind (m/s)
- I(t) Solar Intensity (W/m²)
- L_{ev} Latent heat of vaporization of water (J/kg)
- m_{w} Mass of water in the basin (Kg)
- $d_{w}^{"}$ Water depth in the basin (m)
- t_a Glass cover thickness (m)
- t Time interval (s)
- K_i Thermal conductivity of insulation (W/m°C)
- K_{\perp} Thermal conductivity of glass(W/m°C)
- L_i° Thickness of insulation (m)
- L Thickness of glass (m)
- C_i^s Specific heat of insulation in still (J/kg °C)
- C_w Specific heat of the water in solar still (J/kg °C)
- Partial saturated vapor pressure at a basin water temperature (N/m²)
- P_a Partial saturated vapor pressures at glass cover temperature (N/m²)
- M_{m} Hourly distillate output per unit basin area (l/m²/h)
- M_{uv} Daily distillate output per unit basin area ($l/m^2/d$)

Greek symbols

- α_g Absorptivity of the glass cover
- α_w Absorptivity of the basin water
- α_b Absorptivity of the basin liner
- $\alpha_{\it g}'$ Fraction of solar flux absorbed by a glass cover
- α_w' Fraction of solar flux absorbed by basin water
- α_b' Fraction of solar flux absorbed by basin liner
- $\alpha_{\it eff}$ effective absorptivity
- ε_{g} Emissivity of the glass cover
- ε_w Emissivity of the basin water
- ε_b Emissivity of the basin liner
- $\epsilon_{\it eff}$ $\,$ Effective emissivity between the water surface and glass cover
- σ Stefan-Boltzmann constant
- μ_j Fraction of the solar flux having extinction coeffcient
- η_j Extinction coeffcient

subscripts

- a ambient
- g Glass cover
- w Basin water
- **b** Basin liner
- i internal